

Constraining pseudo-Diracness with astrophysical neutrino flavors

Chee Sheng Fong^{1,*} and Yago Porto^{1,†}

¹*Centro de Ciências Naturais e Humanas,
Universidade Federal do ABC, 09.210-170, Santo André, SP, Brazil*

Abstract

The three Standard Model neutrinos can have Majorana mass or strictly Dirac mass, but both scenarios are practically indistinguishable in neutrino oscillation experiments. If they are pseudo-Dirac, however, there will be new mass splittings among the pseudo-Dirac pairs, potentially leaving traces in neutrino oscillation phenomena. In this work, we use flavor ratios of astrophysical neutrinos to discriminate different possible mass spectra of pseudo-Dirac neutrinos. We show that it will be possible to impose robust bounds of order $\delta m_3^2 \lesssim 10^{-12} \text{ eV}^2$ on the new mass squared splitting involving the third pseudo-Dirac mass eigenstates (those with the least electron flavor composition) with the future experiment IceCube-Gen2. The derived sensitivity is robust because it only assumes an extragalactic origin for the astrophysical neutrinos and hierarchical pseudo-Dirac mass spectrum. In case the neutrino sources are known in the future, such bounds can potentially improve by up to five orders of magnitude, reaching $\delta m_3^2 \lesssim 10^{-17} \text{ eV}^2$.

* sheng.fong@ufabc.edu.br

† yago.porto@ufabc.edu.br

I. INTRODUCTION

Nonzero neutrino mass with at least one mass eigenstate with mass of greater than 0.05 eV has been established experimentally through neutrino oscillation phenomena [1, 2]. In the Standard Model (SM), neutrinos, being electrically neutral, are the only fermions that can acquire Majorana mass without breaking the electromagnetic gauge symmetry. To respect the full SM gauge symmetry, Majorana neutrino mass can only arise from new physics at some scale Λ which breaks the the total lepton number by two units. This leads to neutrinoless double beta decay, which, in the case of an inverted neutrino mass ordering scenario, should be observable in future experiments such as nEXO [3]. On the other hand, if neutrinos were to have Dirac mass, new fermion degrees of freedom (the right-handed neutrinos) have to be introduced. In this case, since lepton number is conserved, neutrinoless double beta decay signature will be absent. In neutrino oscillation experiments where lepton number is conserved, one cannot distinguish between Majorana and Dirac neutrinos. However, if the lepton number is slightly broken such that neutrinos are pseudo-Dirac, there will be new small mass splitting among the pseudo-Dirac pair.¹ While the rate of neutrinoless double beta decay will be suppressed due to small lepton number violation, interestingly, one can probe this scenario in neutrino oscillation experiments as we will discuss next.

In pseudo-Dirac scenario [7], we can have up to three pairs of mass eigenstates ($i = 1, 2, 3$) with squared masses

$$\hat{m}_j^2 = m_j^2 - \frac{1}{2}\delta m_j^2, \quad \hat{m}_{j+3}^2 = m_j^2 + \frac{1}{2}\delta m_j^2, \quad (1)$$

where m_j^2 are the standard mass squared eigenvalues and δm_j^2 are the three new mass squared splittings which have not been observed experimentally and are expected to be smaller than the solar mass splitting. Due to the pseudo-Dirac structure, the mixing between the SM and the right-handed neutrinos are close to maximal. Under the assumption of maximal mixing, strong experimental constraints using solar neutrino data have been derived: $\delta m_{1,2}^2 \lesssim 10^{-11} \text{ eV}^2$, while it is not sensitive to δm_3^2 due to small θ_{13} [4, 8–10]. Using atmospheric, beam and reactor neutrino data which are sensitive to atmospheric mass splitting and θ_{13} , a much weaker constraint is obtained $\delta m_3^2 \lesssim 10^{-5} \text{ eV}^2$ [4]. (See also [8].) Due to the small

¹ The same scenario is referred to as quasi-Dirac in refs. [4–6] but we will opt for pseudo-Dirac, which is a more popular choice in the literature.

mass splitting, astrophysical neutrinos coming from distance sources of Mpc to Gpc allow to probe mass squared difference much smaller than 10^{-12} eV^2 [8, 11–21]. While the pseudo-Diracness of neutrinos are interesting in itself, ref. [6] has showed that it could be linked to the cosmic baryon asymmetry for pseudo-Dirac seesaw model where the new squared mass splitting is intimately connected to the CP violation ϵ required for baryogenesis through leptogenesis as follows²

$$\delta m_i^2 \gtrsim 10^{-8} \text{ eV}^2 \left(\frac{m_i}{0.1 \text{ eV}} \right)^2 \left(\frac{\epsilon}{10^{-7}} \right). \quad (2)$$

Here $\epsilon \sim 10^{-7}$ represents roughly the minimum value required to explain the observed baryon asymmetry. This provides further motivation to explore pseudo-Dirac mass splitting in the above range.

The advent of neutrino telescopes made it possible to study neutrino properties using high-energy (HE) astrophysical neutrinos [23]. Neutrino telescopes employ naturally occurring targets with large volumes to detect tiny astrophysical neutrino fluxes amidst the overwhelming backgrounds of atmospheric neutrinos and muons [24]. The IceCube Neutrino Observatory, for instance, has utilized a cubic kilometer of Antarctic ice since 2011 to observe neutrinos in the TeV–PeV range [25]. Following the discovery of HE neutrinos in 2013 [26, 27], further observations by IceCube [28–34], ANTARES [35], and Baikal-GVD [36] initiated an ongoing phase of characterizing the diffuse neutrino flux and searching for candidate neutrino sources [37–41]. However, despite the recent identification of the first neutrino sources in the northern hemisphere, the origins of most of the diffuse flux are still unknown [42, 43], and the absence of strong anisotropies in the flux indicates an extragalactic origin, with a minor galactic contribution at the level of 10% [44–46].

The extragalactic origin of the HE neutrinos suggests that these particles travel, from their production to detection, a minimum distance of $L \approx 15 \text{ kpc}$, equivalent to the radius of the Milky Way Galaxy. This estimate is notably conservative, considering that the Andromeda Galaxy, the closest major galaxy, lies 600 kpc away, while the nearest Active Galactic Nucleus (NGC5128) is situated roughly 4 Mpc from the Milky Way. This estimate is also compatible with the redshift evolution of BL Lac objects [47, 48]. However, even with such a conservative choice of baseline, we anticipate that IceCube-Gen2 [49] should be

² The pseudo-Dirac leptogenesis model proposed in ref. [22] does not impose such a strong constraint, predicting only a lower bound on seesaw scale for a given pseudo-Dirac mass splitting.

able to impose the constraint $\delta m_3^2 \lesssim 10^{-12} \text{ eV}^2$ due to its improved flavor ratio measurements [50]. This will leverage the constraint on δm_3^2 to the level of the current constraints on $\delta m_{1,2}^2$. On the other hand, in the more optimistic scenario where most potential neutrino sources reside farther away, for example at $z \sim 1$, as suggested by the star-formation rate [48, 51], the bounds would improve: $\delta m_3^2 \lesssim 10^{-17} \text{ eV}^2$.

In this work, we will use astrophysical neutrino flavor ratios to probe pseudo-Dirac neutrinos [11–13, 16]. In this approach, insensitivity to absolute neutrino flux is a double-edged sword. The advantage is that when there exist hierarchies between δm_i^2 , stringent upper bounds on larger δm_i^2 can be derived as we will show in this work. The disadvantage is that if all δm_i^2 ($i = 1, 2, 3$) are of the same order, we will lose the sensitivity. This is to be compared with studies which consider specific astrophysical sources where only certain ranges of δm_i^2 for the first few oscillations can be probed and, away from this region, the analysis is limited by absolute flux uncertainty [17–21]. If the flux from certain source can be determined quite accurately, and in particular, if all δm_i^2 are of the same order, this latter approach is superior. In the view that only very few astrophysical sources are identified, we will focus on flavor ratios approach and see how well this will fare. The paper is organized as follows: in Section II, we will review the parametrization of pseudo-Dirac model at low energy while in Section III, we will discuss the framework to calculate the oscillation probability in this scenario. Then, we will present our main results in Section IV and conclude in Section V.

II. PSEUDO-DIRAC MODEL

If all three SM neutrinos ν_α ($\alpha = e, \mu, \tau$) are pseudo-Dirac in nature, we need to introduce the corresponding right-handed neutrinos ν'_α . (While we have used the same index α , the flavors of ν'_α are arbitrary since they do not feel the SM weak interaction.) After the electroweak symmetry breaking, we can write down the effective neutrino mass term as $\bar{\Psi}^c \mathcal{M} \Psi$ for $\Psi \equiv (\nu_e, \nu_\mu, \nu_\tau, \nu'_e, \nu'_\mu, \nu'_\tau)^T$ with

$$\mathcal{M} = \begin{pmatrix} m_M & m_D \\ m_D^T & m'_M \end{pmatrix}, \quad (3)$$

where the total lepton number is conserved by the Dirac mass term m_D but broken by the Majorana mass terms m_M, m'_M . Without loss of generality, we can work in the basis where

the charged lepton Yukawa is real and diagonal. We define the pseudo-Dirac scenario as when the matrix entries satisfying

$$|m_M|, |m'_M| \ll |m_D|, \quad (4)$$

where the total lepton number is slightly broken.

Let us first look at the Dirac limit, $m_M, m'_M \rightarrow 0$ where the total lepton number is exactly conserved. In this case, m_D can be diagonalized by two unitary matrices U_0 and V_0 as follows

$$\hat{m} = U_0^T m_D V_0 = \text{diag}(m_1, m_2, m_3). \quad (5)$$

Defining

$$\mathcal{U} = \frac{1}{\sqrt{2}} \begin{pmatrix} U_0 & iU_0 \\ V_0 & -iV_0 \end{pmatrix}, \quad (6)$$

\mathcal{M} can be diagonalized as $\mathcal{U}^T \mathcal{M} \mathcal{U} = \text{diag}(\hat{m}, \hat{m})$ where the mass eigenstates are given by

$$\hat{\Psi} = \mathcal{U}^\dagger \Psi \equiv (\nu_1, \nu_2, \nu_3, \nu'_1, \nu'_2, \nu'_3)^T. \quad (7)$$

We can also express the flavor eigenstates in term of the mass eigenstates as

$$\Psi = \mathcal{U} \hat{\Psi} = \frac{1}{\sqrt{2}} \begin{pmatrix} U_0(\nu + i\nu') \\ V_0(\nu - i\nu') \end{pmatrix}, \quad (8)$$

where $\nu \equiv (\nu_1, \nu_2, \nu_3)^T$ and $\nu' \equiv (\nu'_1, \nu'_2, \nu'_3)^T$ pair up to form three Dirac states (*maximal* mixing). Experimentally, only ν_α participate in weak interactions, and hence only U_0 can be measured.

When $m_M, m'_M \neq 0$ but the pseudo-Dirac condition (4) is still satisfied, there will be deviation from eq. (6) and we will have three pairs of pseudo-Dirac mass eigenstates with masses ($j = 1, 2, 3$)

$$\hat{m}_j = m_j - \delta m_j, \quad \hat{m}_{j+3} = m_j + \delta m_j. \quad (9)$$

A useful Euler parametrization for unitary matrix \mathcal{U} is given by

$$\mathcal{U} = \frac{1}{\sqrt{2}} \begin{pmatrix} AU_0 + B & i(AU_0 - B) \\ CU_0 + D & i(CU_0 - D) \end{pmatrix}, \quad (10)$$

where U_0 is a 3×3 unitary matrix while the rest of the 3×3 matrices A , B , C and D are constrained by $\mathcal{U}\mathcal{U}^\dagger = \mathcal{U}^\dagger\mathcal{U} = I_{3 \times 3}$. For example, from $\mathcal{U}\mathcal{U}^\dagger = I_{3 \times 3}$, we have

$$AA^\dagger + BB^\dagger = CC^\dagger + DD^\dagger = I_{3 \times 3}, \quad (11)$$

$$AC^\dagger + BD^\dagger = CA^\dagger + DB^\dagger = 0. \quad (12)$$

In the Dirac limit, $A = I_{3 \times 3}$, $B = C = 0$ and $D = V_0$ and eq. (6) is recovered. Explicitly, we can construct the mixing matrix as

$$\mathcal{U} = U_{\text{new}}UY,$$

where

$$U_{\text{new}} = R_{56}R_{46}R_{36}R_{26}R_{16}R_{45}R_{35}R_{25}R_{15}R_{34}R_{24}R_{14},$$

$$U = R_{23}R_{13}R_{12},$$

and

$$Y \equiv \frac{1}{\sqrt{2}} \begin{pmatrix} I_{3 \times 3} & iI_{3 \times 3} \\ I_{3 \times 3} & -iI_{3 \times 3} \end{pmatrix},$$

with R_{ij} the complex rotation matrix in the ij -plane which can be obtained from a 6×6 identity matrix I by replacing the I_{ii} and I_{jj} by $\cos \theta_{ij}$, I_{ij} by $e^{-i\phi_{ij}} \sin \theta_{ij}$ and I_{ji} by $e^{i\phi_{ij}} \sin \theta_{ij}$. To recover the Dirac limit, we set all the angles in U_{new} (besides θ_{45} , θ_{46} , θ_{56}) to zero. The new angles θ_{45} , θ_{46} , θ_{56} which describe the mixing among the sterile neutrinos (through V_0 in the Dirac limit) are in principle not measurable through the SM interactions.

While the deviation from maximal mixing U_0 is of the order of the following ratios of matrix entries

$$\delta U_0 \sim \frac{|m_M|}{|m_D|}, \frac{|m'_M|}{|m_D|}, \quad (13)$$

the pseudo-Dirac mass squared splittings are of the order of $\delta m_j^2 \sim m_j^2 \delta U_0$. For example, taking $m_j \sim 0.1$ eV and $\delta U_0 \sim 10^{-4}$, the new mass splitting is $\delta m_j^2 \sim 10^{-6}$ eV². So, it is expected that the first discovery of pseudo-Diracness should be through the new mass splittings. In this study, we will assume maximal mixing and focus only on the effects of new mass splittings. We will leave the consideration of deviation from maximal mixing for future study.

III. OSCILLATION PROBABILITY

The amplitude of a neutrino of flavor state ν_α created at $t = 0$ being detected as ν_β at time $t > 0$, $S_{\beta\alpha}(t) \equiv \langle \nu_\beta | \nu_\alpha(t) \rangle$ satisfies the Schrödinger equation

$$i \frac{d}{dt} S(t) = H S(t). \quad (14)$$

The Hamiltonian in the flavor basis is given by

$$H = \mathcal{U} \Delta \mathcal{U}^\dagger + V, \quad (15)$$

where \mathcal{U} is the leptonic mixing matrix, $\Delta \equiv \text{diag}(\hat{m}_1^2, \hat{m}_2^2, \dots)/(2E)$ with E the neutrino energy, and V is the matter potential. For the Pseudo-Dirac model discussed in the previous section, assuming that the ν'_α has no new interactions with the SM, the matter potential for ordinary matter is $V = \text{diag}(V_e - V_n, -V_n, -V_n, 0, 0, 0)$ with $V_e = \sqrt{2}G_F n_e$ and $V_n = G_F n_n/\sqrt{2}$ where G_F is the Fermi constant, and, n_e and n_n are the electron and neutron number density, respectively. The solution to eq. (14) is formally given by

$$S = T \exp \left[-i \int_0^t dt' H(t') \right], \quad (16)$$

where T denotes time ordering.

For astrophysical neutrinos, even if the matter effect is negligible, there is still nontrivial time-dependence due to cosmic expansion. Defining the redshift z as

$$1 + z \equiv \frac{a_0}{a}, \quad (17)$$

where a is the cosmic scale factor with a_0 the value today, we have

$$dt = \frac{dt}{da} da = -\frac{dz}{(1+z)\mathcal{H}}, \quad (18)$$

where $\mathcal{H} \equiv \frac{1}{a} \frac{da}{dt}$ is the Hubble expansion rate which can be expressed in term of current expansion rate \mathcal{H}_0 , total matter fraction Ω_m and dark energy fraction Ω_Λ as follows

$$\mathcal{H}(z) = \mathcal{H}_0 \sqrt{\Omega_m (1+z)^3 + \Omega_\Lambda}. \quad (19)$$

In the above, we have ignored the small radiation density and from the measurements of Planck satellite, we have $\Omega_m = 0.315$, $\Omega_\Lambda = 0.685$ and $\mathcal{H}_0 = 67.4 \text{ km s}^{-1} \text{ Mpc}^{-1}$ [52]. Furthermore, the energy of the neutrino E detected at $z = 0$ will be equal to $E(1+z)$ at

redshift $z > 0$. With negligible matter effect for astrophysical neutrinos $V = 0$, we can write the solution as

$$S_{\beta\alpha} = \sum_j \mathcal{U}_{\beta j} \mathcal{U}_{\alpha j}^* e^{-i \frac{m_j^2}{2E} L_{\text{eff}}}, \quad (20)$$

where we have defined the effective distance as

$$L_{\text{eff}} \equiv c \int_0^z \frac{dz'}{(1+z')^2 \mathcal{H}(z')}, \quad (21)$$

with the speed of light c shown explicitly due to the unit of \mathcal{H}_0 that we have chosen. For $z < 1$, we can Taylor expand in z and obtain at the leading order

$$L_{\text{eff}} \simeq \frac{cz}{\mathcal{H}_0} = 4.4 \text{ Mpc} \left(\frac{z}{0.001} \right) \left(\frac{67.4 \text{ km s}^{-1} \text{ Mpc}^{-1}}{\mathcal{H}_0} \right), \quad (22)$$

where the corrections are $\mathcal{O}(z^2)$. Finally, the transition probability is given by the Born rule $P(\nu_\alpha \rightarrow \nu_\beta) \equiv |S_{\beta\alpha}|^2$.

Assuming the new angles are negligible but new mass splittings are relevant, we have the oscillation probability

$$P(\nu_\alpha \rightarrow \nu_\beta) = \left| \sum_{j=1}^3 U_{0,\beta j} U_{0,\alpha j}^* e^{-i \frac{m_j^2}{2E} L_{\text{eff}}} \cos(\Phi_j) \right|^2, \quad (23)$$

where we have defined

$$\Phi_j \equiv \frac{\delta m_j^2}{4E} L_{\text{eff}}, \quad (24)$$

and used $\delta m_j^2 \simeq 4m_j \delta m_j$ from the definitions in eqs. (1) and (9). Astrophysical neutrino sources are far enough such that we can average out all the standard oscillations involving $m_j^2 - m_k^2 \neq 0$ and obtain

$$P(\nu_\alpha \rightarrow \nu_\beta) \simeq \sum_{j=1}^3 |U_{0,\beta j} U_{0,\alpha j}^*|^2 \cos^2(\Phi_j). \quad (25)$$

If all δm_j^2 are also large enough

$$\Phi_j = 10 \left(\frac{\delta m_j^2}{1.7 \times 10^{-12} \text{ eV}^2} \right) \left(\frac{L_{\text{eff}}}{15 \text{ kpc}} \right) \left(\frac{100 \text{ TeV}}{E} \right) \gg 1, \quad (26)$$

such that we can average out these new oscillations, we obtain

$$P(\nu_\alpha \rightarrow \nu_\beta) \simeq \frac{1}{2} \sum_{j=1}^3 |U_{0,\beta j} U_{0,\alpha j}^*|^2. \quad (27)$$

In general, eq. (27) changes the flux normalization for all flavors. However, if the absolute flux is unknown, it will be challenging to distinguish it from the standard scenario.

On the other hand, using neutrino flavor ratios which do not depend on absolute flux, one can distinguish between the following six cases: Case 1, Case 2, Case 3, Case 12, Case 23, and Case 13 where Case j is defined as $\delta m_{k \neq j}^2 = 0$ and $\Phi_j \gg 1$ with oscillation probability

$$P_{\alpha\beta}^j \equiv \frac{1}{2} |U_{0,\beta j} U_{0,\alpha j}^*|^2 + \sum_{k \neq j} |U_{0,\beta k} U_{0,\alpha k}^*|^2, \quad (28)$$

and Case jk is defined as $\delta m_{l \neq \{j,k\}}^2 = 0$ and $\Phi_{j,k} \gg 1$ with oscillation probability

$$P_{\alpha\beta}^{jk} \equiv \frac{1}{2} |U_{0,\beta j} U_{0,\alpha j}^*|^2 + \frac{1}{2} |U_{0,\beta k} U_{0,\alpha k}^*|^2 + \sum_{l \neq \{j,k\}} |U_{0,\beta l} U_{0,\alpha l}^*|^2. \quad (29)$$

By $\delta m_{k \neq j}^2 = 0$, we mean $\delta m_{k \neq j}^2 \ll \delta m_j^2$ such that oscillations involving $\delta m_{k \neq j}^2$ have not developed.

A. Neutrino flavor ratios

In the standard scenario, the oscillation probability between an initial flavor ν_α to a final flavor ν_β is given by

$$P_{\alpha\beta}^{std} = \sum_{i=1}^3 |U_{\alpha i}|^2 |U_{\beta i}|^2. \quad (30)$$

Therefore, for a flavor composition $(f_{e,S}, f_{\mu,S}, f_{\tau,S})$ at the source S , we can compute the final flavor at the Earth as

$$f_{\beta,\oplus} = \sum_{\alpha=e,\mu,\tau} P_{\alpha\beta}^{std} f_{\alpha,S}. \quad (31)$$

In the presence of averaged-out pseudo-Dirac oscillations, we must change $P_{\alpha\beta}^{std}$ to $P_{\alpha\beta}^j$ or $P_{\alpha\beta}^{jk}$, where the indices j and jk correspond to the pseudo-Dirac scenarios described by eq. (28) and eq. (29). Therefore, for such cases, the final fractions of active flavors ν_β are given by $f_{\beta,\oplus}^j = \sum_\alpha P_{\alpha\beta}^j f_{\alpha,S}$ and $f_{\beta,\oplus}^{jk} = \sum_\alpha P_{\alpha\beta}^{jk} f_{\alpha,S}$, respectively. However, due to the finite conversion probability between active and sterile states, the total flux of active neutrinos will not be conserved from production to detection. Therefore, to determine the detected fractions, we need to normalize $f_{\beta,\oplus}^j$ and $f_{\beta,\oplus}^{jk}$:

$$f_{\beta,\oplus}^{j,\det} = \frac{f_{\beta,\oplus}^j}{f_{e,\oplus}^j + f_{\mu,\oplus}^j + f_{\tau,\oplus}^j} \quad \text{and} \quad f_{\beta,\oplus}^{jk,\det} = \frac{f_{\beta,\oplus}^{jk}}{f_{e,\oplus}^{jk} + f_{\mu,\oplus}^{jk} + f_{\tau,\oplus}^{jk}}. \quad (32)$$

Next, we will focus on the aforementioned six cases and evaluate the sensitivity of IceCube and IceCube-Gen2 in constraining/distinguishing them.

IV. RESULTS

HE astrophysical neutrinos are generated in cosmic particle accelerators when accelerated protons collide with matter (pp interactions) and radiation ($p\gamma$ interactions) [53–57]. These collisions produce mesons, particularly charged pions (π^\pm), which then decay into neutrinos. The decay chain $\pi^- \rightarrow \mu^- + \bar{\nu}_\mu \rightarrow e^- + \bar{\nu}_e + \nu_\mu + \bar{\nu}_\mu$, along with its charge conjugate reaction, produces two muon neutrinos for every electron neutrino: $(1, 2, 0)_S$, where the subscript S denotes the initial proportions at the source³. It is also possible that the decay chain described above is not complete, as the muon may lose energy due to synchrotron emission before decaying. As a result, this will generate the μ -damped scenario, with the proportions $(0, 1, 0)_S$ [63–67]. In this section, however, we assume neutrinos are produced only by the complete chain of π^\pm decay and reach the Earth with averaged-out pseudo-Dirac oscillations, as described by eq. (28) and eq. (29), and compare these scenarios with the standard expectations for both π -decay and μ -damped. More information regarding the μ -damped production combined with the pseudo-Dirac scenario is reserved for the Appendix A.

During propagation from the sources to the Earth, neutrino oscillations modify the initial flavor proportions. In the standard vacuum oscillation scenario, assuming the absence of matter effects [68] and pseudo-Dirac mass splittings, the π^\pm production channel results in flavor equipartition at Earth: $(1 : 2 : 0)_S \rightarrow (1 : 1 : 1)_\oplus$. To be more precise, in fig. 1 and fig. 2, we show the allowed region for the flavor composition at the Earth after considering the 3σ uncertainties of the oscillation parameters [1] where there is no perceptible distinction between normal and inverted mass orderings. Observe that the π -decay (blue region) best fit, in the standard case, is given by $(0.3, 0.36, 0.34)_\oplus$, which lies very close to the benchmark of total flavor equipartition. On the other hand, for the μ -damped case (green region), the best fit is $(0.18, 0.45, 0.37)_\oplus$. Also represented in fig. 1 and fig. 2 are the regions corresponding neutrino flavor at the Earth in the presence of averaged-out pseudo-Dirac oscillation as described by eq. (28) and eq. (29) (red regions). We investigate all possible cases listed in

³ Neutrinos and antineutrinos cannot be distinguished at the IceCube detector. The only exception is the Glashow Resonance [58–61], but it suffers from a lack of statistics, with only one candidate event detected so far [62].

the section III.

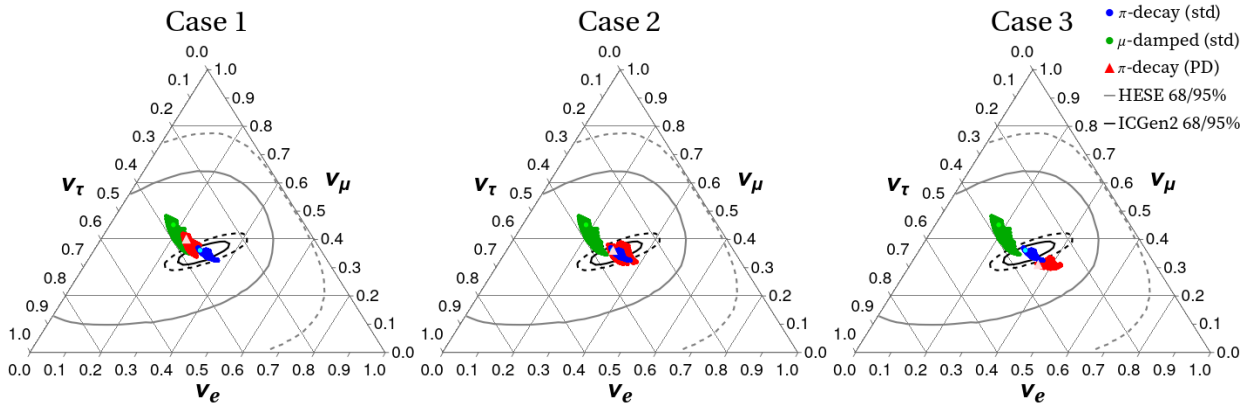


FIG. 1. Expected regions for the flavor composition of HE astrophysical neutrinos, considering the 3σ interval for the oscillation parameters in [1], valid for both normal and inverted mass orderings. The standard (std) expectation for π -decay is shown in blue, the standard μ -damped is shown in green, and the various scenarios for pseudo-Dirac neutrinos are shown in red. In Case j , oscillations corresponding to pseudo-Dirac squared mass splitting δm_j^2 have been averaged out. See the text for more details about the different pseudo-Dirac scenarios.

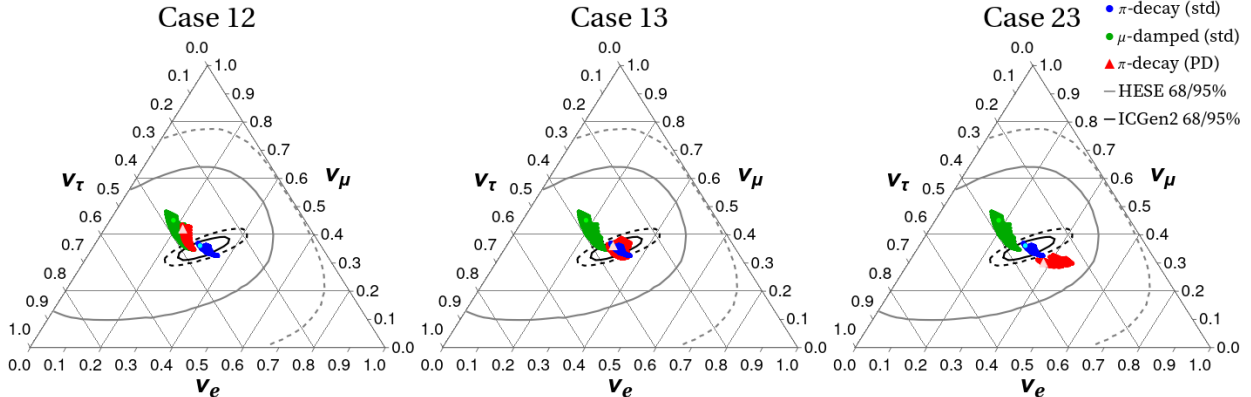


FIG. 2. Same as fig. 1, but for pseudo-Dirac scenarios named Case jk .

We observe that Case 3 and Case 23 stand out as the most distinct from the standard scenarios, even when considering the current uncertainties in the oscillation parameters and production processes (π -decay or μ -damped). What makes the regions corresponding to Cases 3 and 23 so distinct from the standard scenarios is that by decreasing the amount of ν_3 in the flux, we automatically reduce the proportion of $f_{\mu,\oplus}$ (as well as $f_{\tau,\oplus}$, but in a smaller quantity), due to the larger mixing of this propagation eigenstate with ν_μ . Applying the

same reasoning, if some of the ν_1 eigenstates disappear (Case 1 or Case 12), $f_{e,\oplus}$ decreases, and the expected region shifts closer to the typical μ -damped scenario. For Case 13, however, the decrease $f_{\mu\oplus}$ due to the disappearance of ν_3 is balanced by the decrease in $f_{e\oplus}$ resulting from the disappearance of ν_1 , making the final region compatible with the standard π -decay. Moreover, ν_2 has roughly equal mixing with all flavors, so its disappearance (Case 2) has a neutral effect. These results hold true for both normal and inverted mass orderings.

Fig. 1 and fig. 2 also shows the 68% and 95% C.L. contours corresponding to the IceCube analysis [32] of the flavor composition of the HE astrophysical neutrinos using the High-Energy Starting Events (HESE) sample [33]. HESE is an all-flavor, all-sky search using 7.5 years of IceCube data for neutrinos with energies above 60 TeV. Observe that we cannot draw any conclusions from the current HESE bounds, which are still too weak to discriminate even between the standard scenarios. Nevertheless, future detectors, such as IceCube-Gen2 [49], with more statistics and improved capabilities, might significantly enhance the sensitivity to the flavor composition. In fig. 1 and fig. 2 we also show the 68% and 99% projected sensitivities of IceCube-Gen2 after 10 years of observations. The projection of IceCube-Gen2 is taken from [50] and assumes the best fit value to be $(0.3, 0.36, 0.34)_{\oplus}$, compatible with standard π -decay. Observe that with IceCube-Gen2, we can start to distinguish between the standard scenario and some pseudo-Dirac scenarios (Case 3 and Case 23), even if the production process (π -decay and/or μ -damped) remains uncertain at that time. Furthermore, the more precise determination of several oscillation parameters in the next decade will contribute to astrophysical flavor measurements and enhance the discriminatory power of future detectors [69].

V. CONCLUSIONS

In this work, we have shown that using astrophysical neutrino flavor ratios, it is possible to distinguish between six possible cases of pseudo-Dirac neutrino spectra where there exists hierarchies among the new squared mass splitting. In particular, for the case which involves large δm_3^2 in comparison to other pseudo-Dirac mass splittings, a conservative upper bound of order $\delta m_3^2 \lesssim 10^{-12} \text{ eV}^2$ is obtained considering the size of our galaxy and assuming π -decay at neutrino sources with IceCube-Gen2 experiment. From eq. (26), if extragalactic neutrino sources are determined, the bound will greatly improve, up to five orders of magnitude if

the sources are of the distance of Gpc. The benefit of using flavor ratios is its insensitivity to absolute neutrino flux uncertainty while the main caveat is that if all pseudo-Dirac mass splittings are of the same order, one will obtain an overall reduction of flux, making this method futile. As more astrophysical neutrino sources are identified, one can combine the flavor ratio method together with direct measurements to derive the best constraints on pseudo-Dirac neutrinos, exploring completely the window of pseudo-Dirac leptogenesis proposed in ref. [6].

Acknowledgments

YP acknowledges the support by Fundação de Amparo à Pesquisa do Estado de São Paulo (FAPESP) Contract No. 2023/10734-3. CSF acknowledges the support by FAPESP Contracts No. 2019/11197-6, 2022/00404-3, 2023/01467-1 and Conselho Nacional de Desenvolvimento Científico e Tecnológico (CNPq) under Contract No. 304917/2023-0.

Appendix A: μ -damped production combined with pseudo-Dirac scenario

In this section we show the results for the combination of μ -damped production with the pseudo-Dirac scenario. We highlight that only in Case 12 the pseudo-Dirac scenario appears as clearly distinct from standard scenarios, although it will still be hard to discriminate even after 10 years of IceCube-Gen2 operation. As for the pseudo-Dirac scenarios involving ν_3 mass eigenstates (Case 3, Case 13 and Case 23) assuming μ -damped sources, it can result in confusion with the standard scenario assuming π -decay sources.

-
- [1] P. F. de Salas, D. V. Forero, S. Gariazzo, P. Martínez-Miravé, O. Mena, C. A. Ternes, M. Tórtola, and J. W. F. Valle, *JHEP* **02**, 071 (2021), [arXiv:2006.11237 \[hep-ph\]](#).
 - [2] I. Esteban, M. C. Gonzalez-Garcia, M. Maltoni, T. Schwetz, and A. Zhou, *JHEP* **09**, 178 (2020), [arXiv:2007.14792 \[hep-ph\]](#).
 - [3] G. Adhikari *et al.* (nEXO), *J. Phys. G* **49**, 015104 (2022), [arXiv:2106.16243 \[nucl-ex\]](#).
 - [4] G. Anamiati, R. M. Fonseca, and M. Hirsch, *Phys. Rev. D* **97**, 095008 (2018), [arXiv:1710.06249 \[hep-ph\]](#).

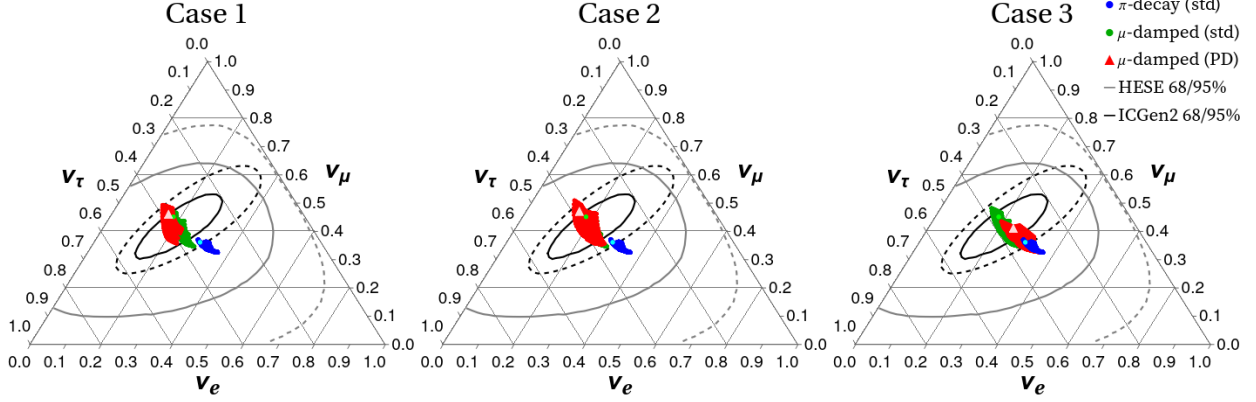


FIG. 3. Same as fig. 1, but with the assumption that pseudo-Dirac neutrinos are produced via the μ -damped channel and corresponding projection of IceCube-Gen2 is taken from [50].

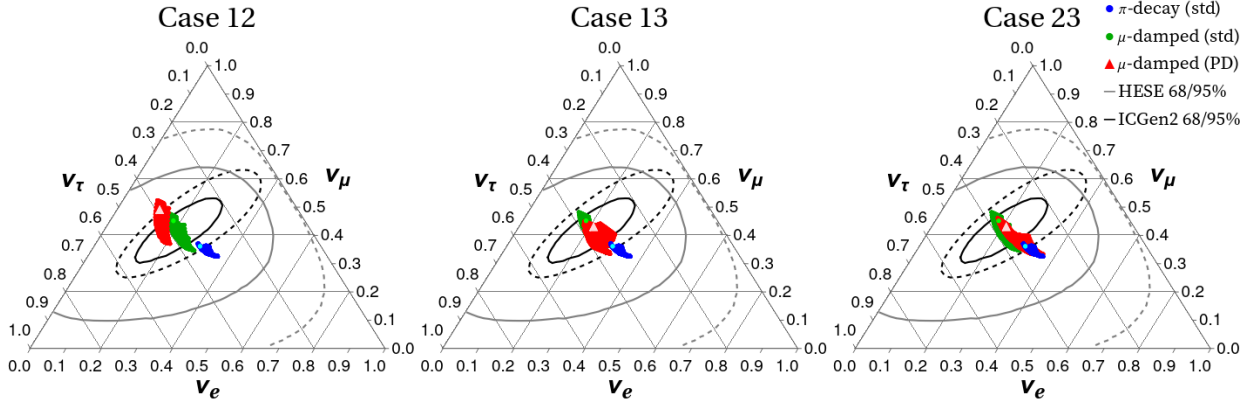


FIG. 4. Same as fig. 2, but with the assumption that pseudo-Dirac neutrinos are produced via the μ -damped channel and corresponding projection of IceCube-Gen2 is taken from [50].

- [5] G. Anamiati, V. De Romeri, M. Hirsch, C. A. Ternes, and M. Tórtola, *Phys. Rev. D* **100**, 035032 (2019), arXiv:1907.00980 [hep-ph].
- [6] C. S. Fong, T. Gregoire, and A. Tonerio, *Phys. Lett. B* **816**, 136175 (2021), arXiv:2007.09158 [hep-ph].
- [7] M. Kobayashi and C. S. Lim, *Phys. Rev. D* **64**, 013003 (2001), arXiv:hep-ph/0012266.
- [8] M. Cirelli, G. Marandella, A. Strumia, and F. Vissani, *Nucl. Phys. B* **708**, 215 (2005), arXiv:hep-ph/0403158.
- [9] A. de Gouvea, W.-C. Huang, and J. Jenkins, *Phys. Rev. D* **80**, 073007 (2009), arXiv:0906.1611 [hep-ph].
- [10] S. Ansarifard and Y. Farzan, *Phys. Rev. D* **107**, 075029 (2023), arXiv:2211.09105 [hep-ph].

- [11] P. Keranen, J. Maalampi, M. Myyrylainen, and J. Riittinen, *Phys. Lett. B* **574**, 162 (2003), [arXiv:hep-ph/0307041](#).
- [12] J. F. Beacom, N. F. Bell, D. Hooper, J. G. Learned, S. Pakvasa, and T. J. Weiler, *Phys. Rev. Lett.* **92**, 011101 (2004), [arXiv:hep-ph/0307151](#).
- [13] A. Esmaili, *Phys. Rev. D* **81**, 013006 (2010), [arXiv:0909.5410 \[hep-ph\]](#).
- [14] A. Esmaili and Y. Farzan, *JCAP* **12**, 014 (2012), [arXiv:1208.6012 \[hep-ph\]](#).
- [15] A. S. Joshipura, S. Mohanty, and S. Pakvasa, *Phys. Rev. D* **89**, 033003 (2014), [arXiv:1307.5712 \[hep-ph\]](#).
- [16] V. Brdar and R. S. L. Hansen, *JCAP* **02**, 023 (2019), [arXiv:1812.05541 \[hep-ph\]](#).
- [17] A. De Gouvêa, I. Martinez-Soler, Y. F. Perez-Gonzalez, and M. Sen, *Phys. Rev. D* **102**, 123012 (2020), [arXiv:2007.13748 \[hep-ph\]](#).
- [18] I. Martinez-Soler, Y. F. Perez-Gonzalez, and M. Sen, *Phys. Rev. D* **105**, 095019 (2022), [arXiv:2105.12736 \[hep-ph\]](#).
- [19] T. Rink and M. Sen, *Phys. Lett. B* **851**, 138558 (2024), [arXiv:2211.16520 \[hep-ph\]](#).
- [20] K. Carloni, I. Martínez-Soler, C. A. Argüelles, K. S. Babu, and P. S. B. Dev, *Phys. Rev. D* **109**, L051702 (2024), [arXiv:2212.00737 \[astro-ph.HE\]](#).
- [21] K. Dixit, L. S. Miranda, and S. Razzaque, (2024), [arXiv:2406.06476 \[astro-ph.HE\]](#).
- [22] Y. H. Ahn, S. K. Kang, and C. S. Kim, *JHEP* **10**, 092 (2016), [arXiv:1602.05276 \[hep-ph\]](#).
- [23] S. Pakvasa, *Mod. Phys. Lett. A* **19**, 1163 (2004), [arXiv:hep-ph/0405179](#).
- [24] C. A. Argüelles, F. Halzen, and N. Kurahashi, (2024), [arXiv:2405.17623 \[hep-ex\]](#).
- [25] M. Ahlers and F. Halzen, *Prog. Part. Nucl. Phys.* **102**, 73 (2018), [arXiv:1805.11112 \[astro-ph.HE\]](#).
- [26] M. G. Aartsen *et al.* (IceCube), *Phys. Rev. Lett.* **111**, 021103 (2013), [arXiv:1304.5356 \[astro-ph.HE\]](#).
- [27] M. G. Aartsen *et al.* (IceCube), *Science* **342**, 1242856 (2013), [arXiv:1311.5238 \[astro-ph.HE\]](#).
- [28] M. G. Aartsen *et al.* (IceCube), *Phys. Rev. Lett.* **113**, 101101 (2014), [arXiv:1405.5303 \[astro-ph.HE\]](#).
- [29] M. G. Aartsen *et al.* (IceCube), *Astrophys. J.* **809**, 98 (2015), [arXiv:1507.03991 \[astro-ph.HE\]](#).
- [30] M. G. Aartsen *et al.* (IceCube), *Phys. Rev. Lett.* **115**, 081102 (2015), [arXiv:1507.04005 \[astro-ph.HE\]](#).
- [31] M. G. Aartsen *et al.* (IceCube), *Astrophys. J.* **833**, 3 (2016), [arXiv:1607.08006 \[astro-ph.HE\]](#).

- [32] R. Abbasi *et al.* (IceCube), *Eur. Phys. J. C* **82**, 1031 (2022), arXiv:2011.03561 [hep-ex].
- [33] R. Abbasi *et al.* (IceCube), *Phys. Rev. D* **104**, 022002 (2021), arXiv:2011.03545 [astro-ph.HE].
- [34] R. Abbasi *et al.* (IceCube), *Astrophys. J.* **928**, 50 (2022), arXiv:2111.10299 [astro-ph.HE].
- [35] A. Albert *et al.* (ANTARES), *Astrophys. J. Lett.* **853**, L7 (2018), arXiv:1711.07212 [astro-ph.HE].
- [36] V. A. Allakhverdyan *et al.* (Baikal-GVD), *Phys. Rev. D* **107**, 042005 (2023), arXiv:2211.09447 [astro-ph.HE].
- [37] M. G. Aartsen *et al.* (IceCube), *Science* **361**, 147 (2018), arXiv:1807.08794 [astro-ph.HE].
- [38] M. G. Aartsen *et al.* (IceCube, Fermi-LAT, MAGIC, AGILE, ASAS-SN, HAWC, H.E.S.S., INTEGRAL, Kanata, Kiso, Kapteyn, Liverpool Telescope, Subaru, Swift NuSTAR, VERITAS, VLA/17B-403), *Science* **361**, eaat1378 (2018), arXiv:1807.08816 [astro-ph.HE].
- [39] X. Rodrigues, S. Garrappa, S. Gao, V. S. Paliya, A. Franckowiak, and W. Winter, *Astrophys. J.* **912**, 54 (2021), arXiv:2009.04026 [astro-ph.HE].
- [40] R. Abbasi *et al.* (IceCube), *Science* **378**, 538 (2022), arXiv:2211.09972 [astro-ph.HE].
- [41] A. Albert *et al.* (ANTARES, OVRO), *Astrophys. J.* **964**, 3 (2024), arXiv:2309.06874 [astro-ph.HE].
- [42] N. Kurahashi, K. Murase, and M. Santander, *Ann. Rev. Nucl. Part. Sci.* **72**, 365 (2022), arXiv:2203.11936 [astro-ph.HE].
- [43] S. Troitsky, *Usp. Fiz. Nauk* **194**, 371 (2024), arXiv:2311.00281 [astro-ph.HE].
- [44] M. Ahlers, Y. Bai, V. Barger, and R. Lu, *Phys. Rev. D* **93**, 013009 (2016), arXiv:1505.03156 [hep-ph].
- [45] R. Abbasi *et al.* (IceCube), *Science* **380**, adc9818 (2023), arXiv:2307.04427 [astro-ph.HE].
- [46] M. Bustamante, *Nature Rev. Phys.* **6**, 8 (2024), arXiv:2312.08102 [astro-ph.HE].
- [47] M. Ajello *et al.*, *Astrophys. J.* **780**, 73 (2014), arXiv:1310.0006 [astro-ph.CO].
- [48] A. Capanema, A. Esmaili, and P. D. Serpico, *JCAP* **02**, 037 (2021), arXiv:2007.07911 [hep-ph].
- [49] M. G. Aartsen *et al.* (IceCube-Gen2), *J. Phys. G* **48**, 060501 (2021), arXiv:2008.04323 [astro-ph.HE].
- [50] R. Abbasi *et al.* (IceCube-Gen2), *PoS ICRC2023*, 1123 (2023), arXiv:2308.15220 [astro-ph.HE].
- [51] A. M. Hopkins and J. F. Beacom, *Astrophys. J.* **651**, 142 (2006), arXiv:astro-ph/0601463.

- [52] N. Aghanim *et al.* (Planck), *Astron. Astrophys.* **641**, A6 (2020), [Erratum: *Astron.Astrophys.* 652, C4 (2021)], [arXiv:1807.06209 \[astro-ph.CO\]](#).
- [53] S. H. Margolis, D. N. Schramm, and R. Silberberg, *Astrophys. J.* **221**, 990 (1978).
- [54] F. W. Stecker, *Astrophys. J.* **228**, 919 (1979).
- [55] A. Mucke, R. Engel, J. P. Rachen, R. J. Protheroe, and T. Stanev, *Comput. Phys. Commun.* **124**, 290 (2000), [arXiv:astro-ph/9903478](#).
- [56] S. R. Kelner, F. A. Aharonian, and V. V. Bugayov, *Phys. Rev. D* **74**, 034018 (2006), [Erratum: *Phys.Rev.D* 79, 039901 (2009)], [arXiv:astro-ph/0606058](#).
- [57] S. Hummer, M. Ruger, F. Spanier, and W. Winter, *Astrophys. J.* **721**, 630 (2010), [arXiv:1002.1310 \[astro-ph.HE\]](#).
- [58] S. L. Glashow, *Phys. Rev.* **118**, 316 (1960).
- [59] A. Bhattacharya, R. Gandhi, W. Rodejohann, and A. Watanabe, *JCAP* **10**, 017 (2011), [arXiv:1108.3163 \[astro-ph.HE\]](#).
- [60] G.-y. Huang, M. Lindner, and N. Volmer, *JHEP* **11**, 164 (2023), [arXiv:2303.13706 \[hep-ph\]](#).
- [61] Q. Liu, N. Song, and A. C. Vincent, *Phys. Rev. D* **108**, 043022 (2023), [arXiv:2304.06068 \[astro-ph.HE\]](#).
- [62] M. G. Aartsen *et al.* (IceCube), *Nature* **591**, 220 (2021), [Erratum: *Nature* 592, E11 (2021)], [arXiv:2110.15051 \[hep-ex\]](#).
- [63] J. P. Rachen and P. Meszaros, *Phys. Rev. D* **58**, 123005 (1998), [arXiv:astro-ph/9802280](#).
- [64] T. Kashti and E. Waxman, *Phys. Rev. Lett.* **95**, 181101 (2005), [arXiv:astro-ph/0507599](#).
- [65] M. Kachelriess, S. Ostapchenko, and R. Tomas, *Phys. Rev. D* **77**, 023007 (2008), [arXiv:0708.3047 \[astro-ph\]](#).
- [66] S. Hummer, M. Maltoni, W. Winter, and C. Yaguna, *Astropart. Phys.* **34**, 205 (2010), [arXiv:1007.0006 \[astro-ph.HE\]](#).
- [67] W. Winter, *Phys. Rev. D* **90**, 103003 (2014), [arXiv:1407.7536 \[astro-ph.HE\]](#).
- [68] P. S. B. Dev, S. Jana, and Y. Porto, (2023), [arXiv:2312.17315 \[hep-ph\]](#).
- [69] N. Song, S. W. Li, C. A. Argüelles, M. Bustamante, and A. C. Vincent, *JCAP* **04**, 054 (2021), [arXiv:2012.12893 \[hep-ph\]](#).